Results on Neutrino Non-Standard Interactions with KM3NeT/ORCA6 and ANTARES

Alfonso Lazo Pedrajas
on behalf of the KM3NeT and ANTARES Collaborations

IFIC-Instituto de Física Corpuscular (CSIC-Universitat de València)
XVIII International Conference on Topics in Astroparticle and Underground Physics

31/08/2023

Non-Standard Interactions

- NSIs appear naturally in several extensions of the Standard Model (SM) which try to provide mechanisms for the origin of neutrino masses.
- NC NSIs would affect neutrino oscillations in matter through coherent forward scattering.
- Atmospheric ν experiements are most sensitive to $\varepsilon_{\mu\tau}$ and $\varepsilon_{\tau\tau} - \varepsilon_{\mu\mu}$, followed by $\varepsilon_{e\tau}$ and $\varepsilon_{e\mu}$.

$$\mathcal{L}_{\text{NSI}}^{\text{NC}} = -2\sqrt{2} G_F \varepsilon_{\alpha\beta}^{fL,R} \left(\bar{\nu}_\alpha \gamma_\mu P_L \nu_\beta\right) \left(\bar{f} \gamma^\mu P_{L,R} f\right)$$

$$\mathcal{H}_{\text{eff}} = \tfrac{1}{2E} U_{PMNS} \begin{bmatrix} 0 & 0 & 0 \\ 0 & \Delta m^2_{21} & 0 \\ 0 & 0 & \Delta m^2_{31} \end{bmatrix} U^{+}_{PMNS} + A(x) \begin{bmatrix} 1+\varepsilon_{ee} & \varepsilon_{e\mu} & \varepsilon_{e\tau} \\ \varepsilon^*_{e\mu} & \varepsilon_{\mu\mu} & \varepsilon_{\mu\tau} \\ \varepsilon^*_{e\tau} & \varepsilon^*_{\mu\tau} & \varepsilon_{\tau\tau} \end{bmatrix}, \quad A(x) = \sqrt{2} G_F n_e(x)$$

Non-Standard Interactions

- NSIs coupling strengths inspected ony by one. They give rise to a rich phenomenology.
- Difference in $P_{\mu\mu}$ between standard oscillations and different realizations of NSIs coupling strengths.

$$\mathcal{H}_{\rm nsi} = A(x) \begin{bmatrix} \varepsilon_{ee} & \varepsilon_{e\mu} & \varepsilon_{e\tau} \\ \varepsilon^*_{e\mu} & \varepsilon_{\mu\mu} & \varepsilon_{\mu\tau} \\ \varepsilon^*_{e\tau} & \varepsilon^*_{\mu\tau} & \varepsilon_{\tau\tau} \end{bmatrix}$$

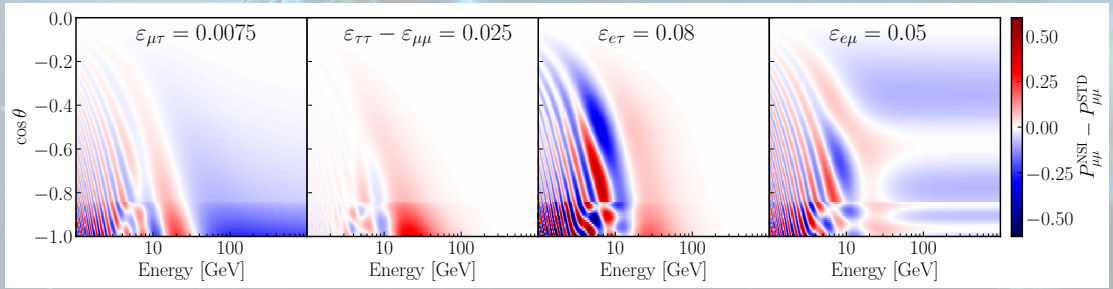

KM3NeT/ORCA6 and ANTARES

ANTARES

- 25 storeys with 3 single-PMT Optical Modules (OMs).
- 12 detection lines from 2008, decommissioned in 2022.
- $\sim$ 70m horizontal line spacing, $\sim$ 14.5m vertical storey spacing.
- **Detection of high-energy neutrinos.**

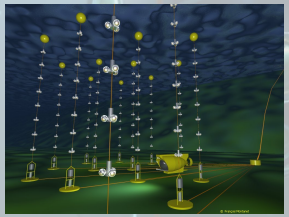

KM3NeT/ORCA

- 18 Multi-PMT Digital Optical Modules (DOMs) along vertical Detection Units (DUs).
- 18 DUs deployed out of 115 foreseen.
- $\sim$ 20m horizontal DU spacing, $\sim$ 9m vertical DOM spacing.
- **Measurement of Neutrino Mass Ordering and neutrino oscillation parameters.**

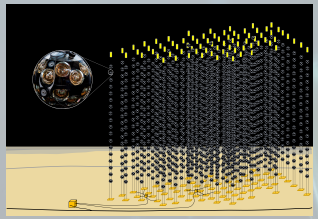

KM3NeT/ORCA6 dataset

- First configuration of ORCA with 6 DUs (January 20- November 21).
- **433 kton-yr** of exposure after run selection:
  - Strict quality criteria on environmental conditions.
  - Stability of the data taking.
- Filtering of pure noise events based on reconstruction quality and trigger conditions.
- BDTs used to discriminate **neutrino vs atm. muon** and **track vs shower**.
- Three PID classes, approximately equally populated.

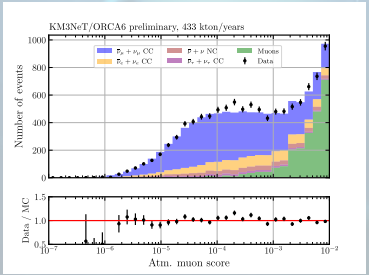

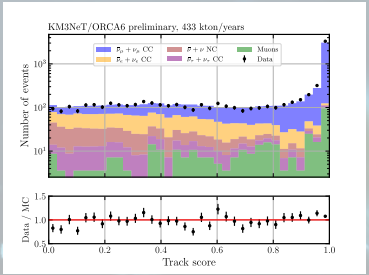

KM3NeT/ORCA6 dataset

- **High purity tracks** with 95% $\nu_\mu/\bar{\nu}_\mu$-CC, $< 1\%$ atm. μ.
- **Low purity tracks** with 90% $\nu_\mu/\bar{\nu}_\mu$-CC, 4% atm. μ.
- **Showers** with 46% $\nu_\mu/\bar{\nu}_\mu$-CC, 1% atm. μ.

- High purity tracks bring the highest sensitivity to ν oscillations.
- Low purity tracks help constraining systematics.

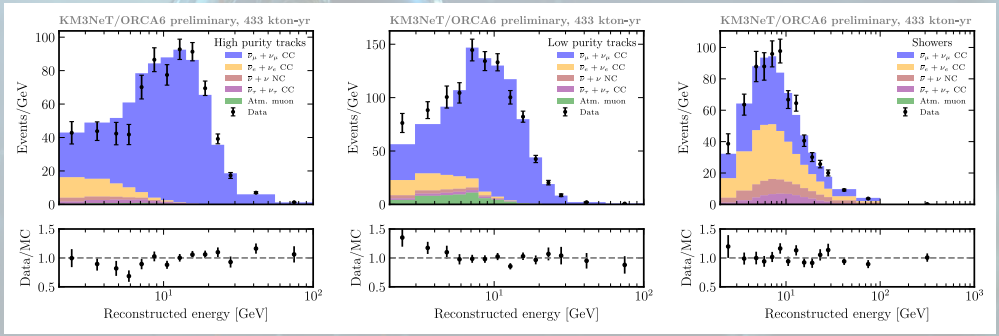

ANTARES dataset

- Dataset from 2007 to 2016. **2830** days of livetime analysed.
- **7710** events selected into a single track-like class.
- Event selection based on previous ANTARES oscillation analysis 10.1007/JHEP06(2019)113.

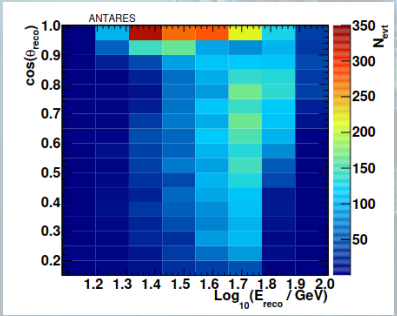

- Single-line and multi-line event reconstruction.
- Reconstructed energies from 16 GeV to 100 GeV.
- NSI sensitivity from bulk of statistics with high energy ν migration.
- Published results 10.1007/JHEP07(2022)048

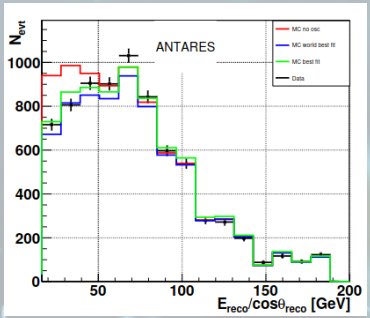

Analysis method

- Maximum Likelihood Estimation of the parameters:

$$-2\log\mathcal{L} = \left\{ 2\sum_{i,j}^{bins}\left[N_{ij}^{m}(\vec{\omega},\vec{\eta}) - N_{ij}^{\mathrm{dat}} + N_{ij}^{\mathrm{dat}}\log\left(\frac{N_{ij}^{\mathrm{dat}}}{N_{ij}^{m}(\vec{\omega},\vec{\eta})}\right)\right] + \sum_{k}^{syst.}\left(\frac{\eta_k - \langle\eta_k\rangle}{\sigma_k}\right)^2 \right\} .$$

- Profiled likelihood scans of the NSIs parameters, one by one:
  $-2\log(\mathcal{L}_{NSIs}/\mathcal{L}_{bf}) = -2\Delta\log\mathcal{L}$.
- Binning in PID$\times \log(E_{\mathrm{rec}}/\mathrm{GeV}) \times \cos\theta_z$
- 3 PID bins x 15x10 binning for **ORCA6**
- 1 PID bin x 8x17 for **ANTARES**

- Uncertainties in flux, detector, cross-section and background modelling in **ORCA6**.

	Nominal value	Syst. unc.
$\Delta m^2_{31}\cdot 10^{-3}$ [eV^2]	2.517 (NO) /-2.424 (IO)	free
$\Delta m^2_{21}\cdot 10^{-5}$ [eV^2]	7.42	fixed
θ_{23} [°]	49.2 (NO) / 49.3 (IO)	free
θ_{21} [°]	33.44	fixed
θ_{31} [°]	8.57 (NO) / 8.60 (IO)	fixed
High purity Normalisation	1.0	free
Overall Normalisation	1.0	free
Shower Normalisation	1.0	free
Atm. Muon Normalisation	1.0	free
HE Light Sim	1.0	50%
Energy Scale	1.0	9%
Flux energy slope	0.0	10%
Flux zenith slope	0.0	2%
ν_τ Normalisation	1.0	20%
ν NC Normalisation	1.0	20%
$\nu_\mu/\bar{\nu}_\mu$	0.0	5%
$\nu_e/\bar{\nu}_e$	0.0	7%
ν_μ/ν_e	0.0	2%

Results: $\varepsilon_{\mu\tau}$ and $\varepsilon_{\tau\tau} - \varepsilon_{\mu\mu}$

- Complex NSIs strengths explored in ORCA6.
- Correlated real valued $\varepsilon_{\mu\tau}$ vs $\varepsilon_{\tau\tau} - \varepsilon_{\mu\mu}$ in ANTARES.

- **No significant deviation from standard interactions** found in the datasets.

	Hypothesis	Best fit	p-value
ORCA6	$\lvert\varepsilon_{\mu\tau}\rvert,\ \delta_{\mu\tau}$	$1^{+3}_{-1} \cdot 10^{-3},\ (0^{+360}_{-0})^\circ$	0.66
	$\varepsilon_{\tau\tau} - \varepsilon_{\mu\mu}$	$(0 \pm 1) \cdot 10^{-2}$	0.90
	$\lvert\varepsilon_{e\tau}\rvert,\ \delta_{e\tau}$	$(4 \pm 3) \cdot 10^{-2},\ (190 \pm 70)^\circ$	0.23
	$\lvert\varepsilon_{e\mu}\rvert,\ \delta_{e\mu}$	$(3 \pm 2) \cdot 10^{-2},\ (140 \pm 70)^\circ$	0.25
ANTARES	$\varepsilon_{\mu\tau}$	$(-1 \pm 2) \cdot 10^{-3}$	0.09
	$\varepsilon_{\tau\tau} - \varepsilon_{\mu\mu}$	$0.032^{+0.014}_{-0.008}$	

10.1007/JHEP07(2022)048

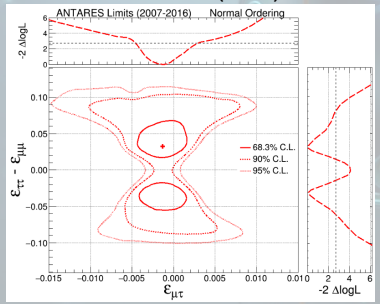

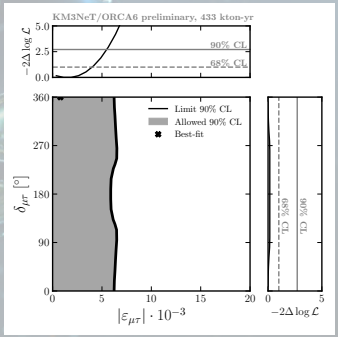

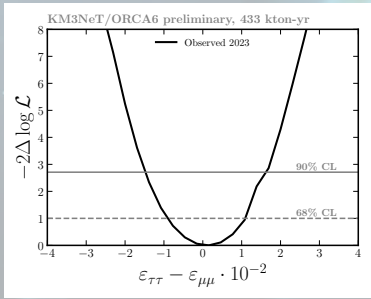

Results: $\varepsilon_{e\tau}$ and $\varepsilon_{e\mu}$

- **ORCA6** can additionally constrain $\varepsilon_{e\tau}$ and $\varepsilon_{e\mu}$.
- Significant contribution to $|\varepsilon_{e\tau}|$ and $|\varepsilon_{e\mu}|$ sensitivity from shower class.
- No sensitivity to the complex phases at 90% CL.

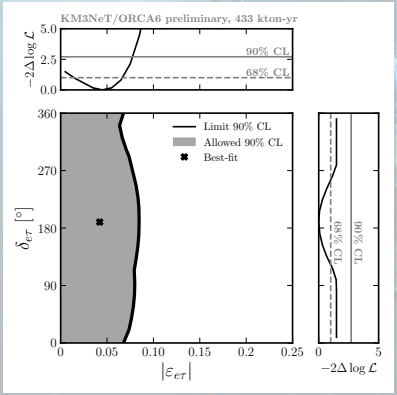

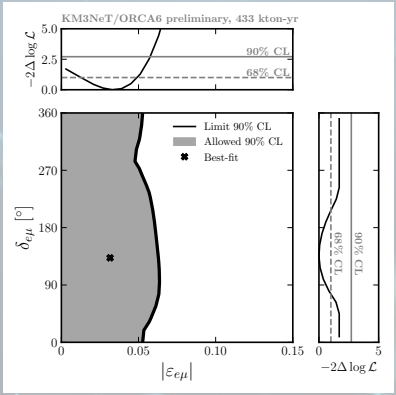

Likelihood ratio maps ORCA6

- Maps show $-2\log(\mathcal{L}_{90\%}/\mathcal{L}_{BF})$ for each NSIs hypothesis.
- Most important contribution from **high purity track** class.
- Sensitivity to $\varepsilon_{\mu\tau}$ and $\varepsilon_{e\mu}$ arising from high-energy ν migration.
- $\varepsilon_{e\tau}$ and $\varepsilon_{\tau\tau} - \varepsilon_{\mu\mu}$ sensitivity mostly at oscillation valley.

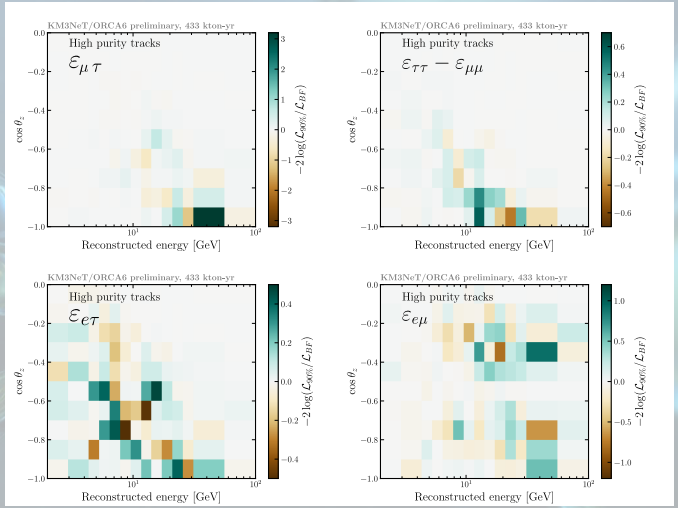

Best-fit distributions in ORCA6

- Reconstructed $cos\theta_z$ transformed into baseline and divided by reconstructed energy.
- Distributions normalised to the no-oscillation case.
- Small NSIs pulls $\rightarrow$ NSIs best-fit distributions follow closely the standard oscillation case.
- NSI 5 σ strength shown for comparison.

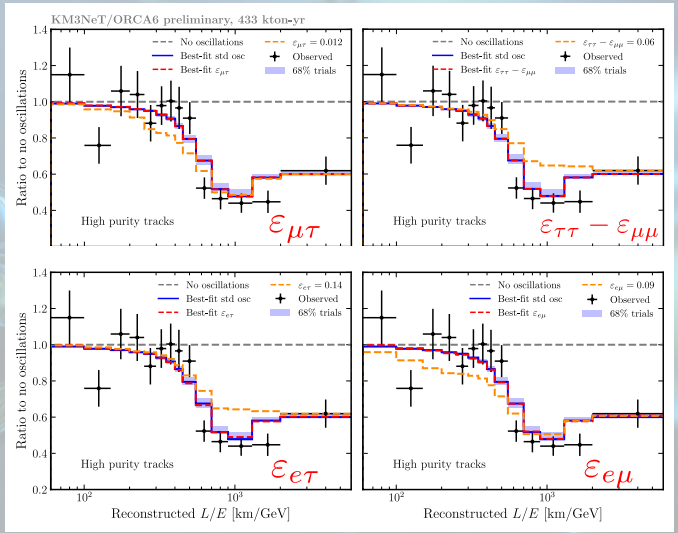

Summary & comparison to other experiments

ANTARES 90% CL limits

$$-4.7 \cdot 10^{-3} \leq \varepsilon_{\mu\tau} \leq 4.7 \cdot 10^{-3}$$
$$-6.4 \cdot 10^{-2} \leq \varepsilon_{\tau\tau} - \varepsilon_{\mu\mu} \leq -0.4 \cdot 10^{-2}$$
$$\cup$$
$$1.4 \cdot 10^{-2} \leq \varepsilon_{\tau\tau} - \varepsilon_{\mu\mu} \leq 8.1 \cdot 10^{-2}$$

Real-valued allowed regions, both orderings profiled

ORCA6 90% CL limits

$$-4.7 \cdot 10^{-3} \leq \varepsilon_{\mu\tau} \leq 5.2 \cdot 10^{-3}$$
$$-1.5 \cdot 10^{-2} \leq \varepsilon_{\tau\tau} - \varepsilon_{\mu\mu} \leq 1.6 \cdot 10^{-2}$$
$$-7.7 \cdot 10^{-2} \leq \varepsilon_{e\tau} \leq 2.8 \cdot 10^{-2}$$
$$-5.6 \cdot 10^{-2} \leq \varepsilon_{e\mu} \leq 4.3 \cdot 10^{-2}$$

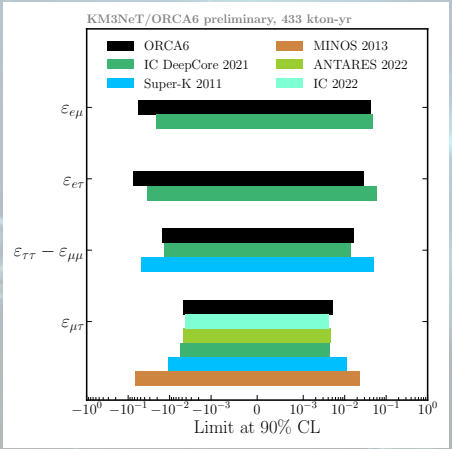

Conclusions

- **ANTARES** placed competitive bounds on $\varepsilon_{\mu\tau}$ with **10 years** of exposure.
- Constrains have been placed on four NSIs parameters using **433 kton-yr** of **ORCA6**.
- **ORCA6** analysis benefits from extended exposure, improved selection and reconstruction techniques compared to previous works.

- There is room for potential improvement coming mainly from **extended instrumented volume** and **increased total exposure**.

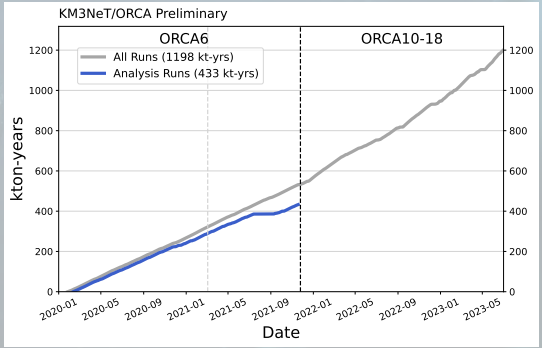

Backup

Backup: nuisance parameter impact ORCA6

- Nuisance parameters are shifted $\pm\sigma$ away from its best fit while fitting the remaining systematics.
- The shift induced in NSIs absolute value is normalised to its uncertainty $(|\varepsilon^{\text{shift}}| - |\varepsilon^{\text{BF}}|)/\sigma_\varepsilon$.
- Upper scale: pulls, lower scale: shifts in $\varepsilon_{\alpha\beta}$.

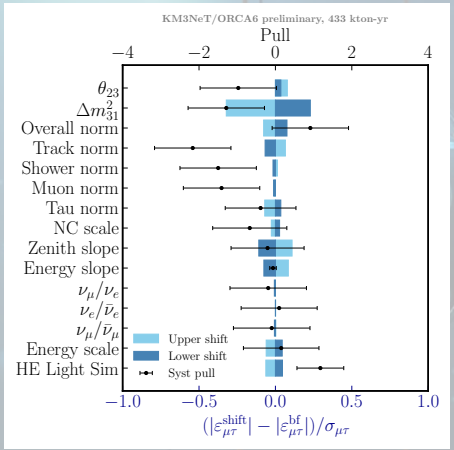

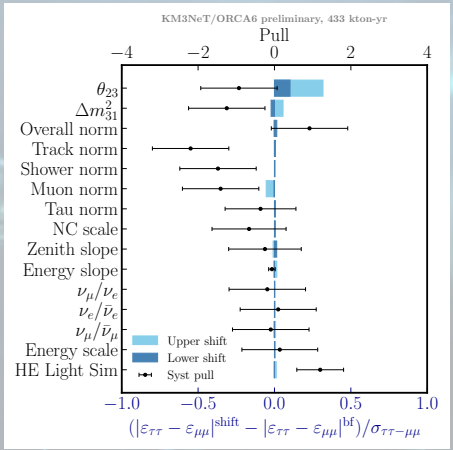

Backup: nuisance parameter impact ORCA6

- Nuisance parameters are shifted $\pm\sigma$ away from its best fit while fitting the remaining systematics.
- The shift induced in NSIs absolute value is normalised to its uncertainty $(|\varepsilon^{\text{shift}}| - |\varepsilon^{\text{BF}}|)/\sigma_\varepsilon$.
- Upper scale: pulls, lower scale: shifts in $\varepsilon_{\alpha\beta}$.

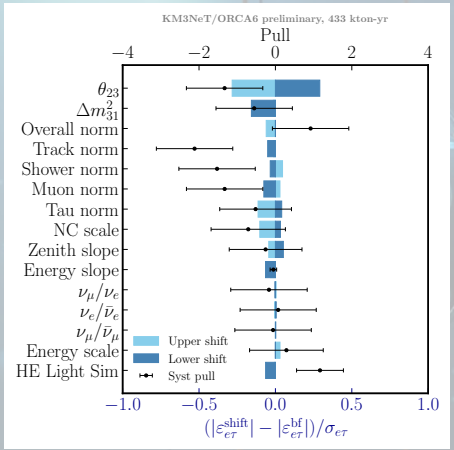

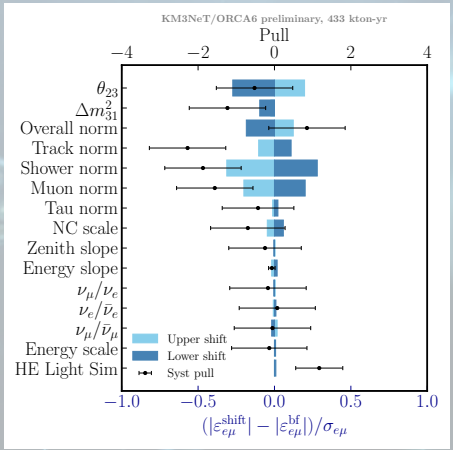

Backup

- Comparison with Asimov sensitivity.

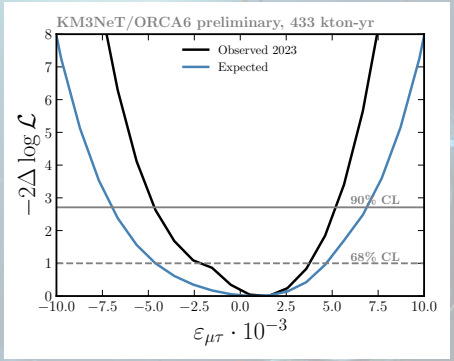

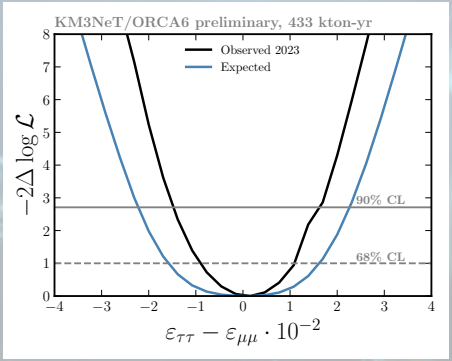

Backup

- Comparison with Asimov sensitivity.

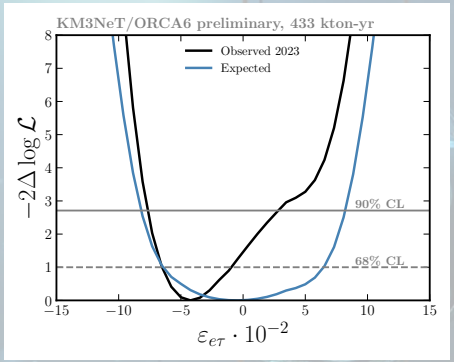

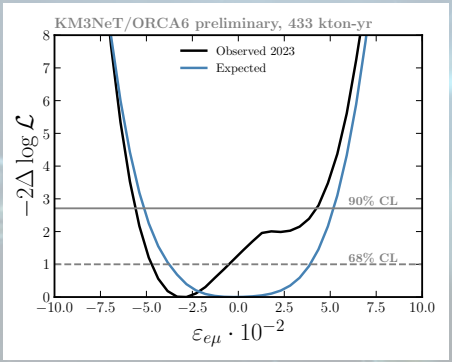

Backup

- Zenith angle distribution for the high purity track class, divided into four energy slices. The NSI best fit is shown for $\varepsilon_{\mu\tau}$ (red), together with the standard oscillation best fit (blue) and the distribution obtained from shifting $\varepsilon_{\mu\tau}$ 5σ away from zero (yelllow).

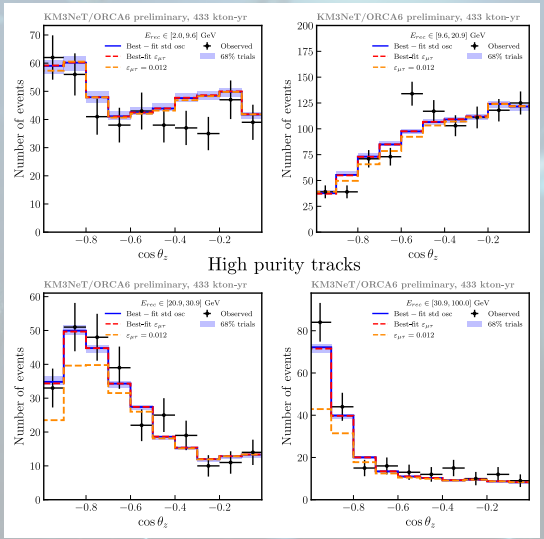

Backup

- Zenith angle distribution for the high purity track class, divided into four energy slices. The NSI best fit is shown for $\varepsilon_{\tau\tau} - \varepsilon_{\mu\mu}$ (red), together with the standard oscillation best fit (blue) and the distribution obtained from shifting $\varepsilon_{\tau\tau} - \varepsilon_{\mu\mu}$ 5σ away from zero (yelllow).

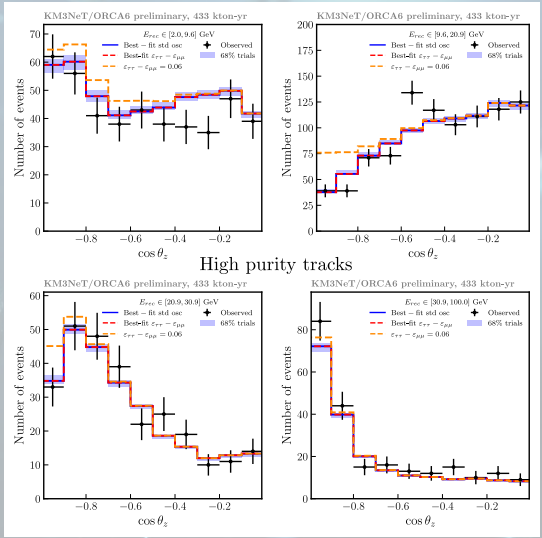

Backup

- Zenith angle distribution for the high purity track class, divided into four energy slices. The NSI best fit is shown for $\varepsilon_{e\tau}$ (red), together with the standard oscillation best fit (blue) and the distribution obtained from shifting $\varepsilon_{e\tau}$ 5σ away from zero (yelllow).

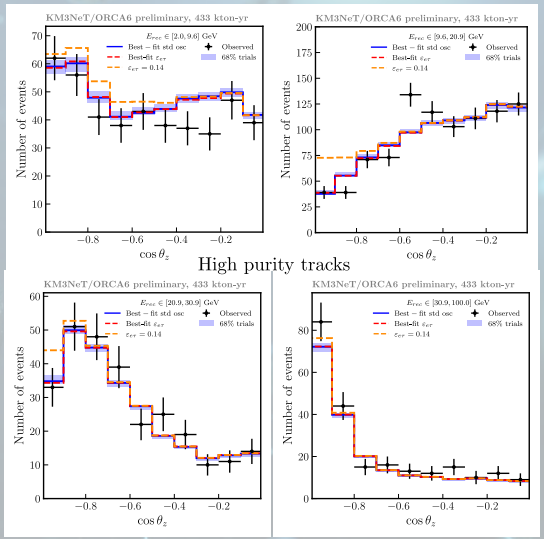

Backup

- Zenith angle distribution for the high purity track class, divided into four energy slices. The NSI best fit is shown for $\varepsilon_{e\mu}$ (red), together with the standard oscillation best fit (blue) and the distribution obtained from shifting $\varepsilon_{e\mu}$ 5σ away from zero (yelllow).